

# Momentum Integral Methods for the Laminar Free Shear Layer

TOSHI KUBOTA\* AND C. FORBES DEWEY JR †  
*California Institute of Technology, Pasadena, Calif*

A momentum integral technique is used to describe the nonsimilar growth of the constant pressure laminar free shear layer with finite initial thickness. An essential feature of the analysis is the division of the shear layer into two parts, one above and one below the zero streamline. Separate polynomial or exponential profiles are used to represent the velocity profile in each part; suitable matching conditions lead to closed form solutions of the momentum equation with simple expressions for velocity profiles. Use of the Howarth transformation allows a description of the effects of Mach number and boundary temperature on the growth of the shear layer and the Mach number  $M_*$  along the dividing streamline.

## Formulation of the Problem

**M**OMENTUM integral methods are very convenient for treating a wide variety of separated flow problems. Several examples have been reported in the literature<sup>1-3</sup> and further applications are being pursued.<sup>6,7</sup> For the constant pressure mixing problem, the application is simple and direct, and leads to closed form solutions of the momentum equation with simple profiles. This paper describes the development of a constant pressure laminar free mixing layer with a finite initial thickness.

We assume that the usual boundary-layer approximations are valid in the mixing layer, and the Howarth transformation is used to reduce the equations to incompressible form (unbarred variables are in the transformed plane):

$$s = \bar{s} \quad y = \int_0^{\bar{y}} \left( \frac{\rho}{\rho_e} \right) d\bar{y} \quad (1)$$

where  $\bar{s}$  is the distance measured along the dividing streamline, and  $\bar{y}$  is the distance normal to the dividing streamline. Defining the stream function  $\psi$  in the usual manner,

$$\rho \bar{u} = \rho (\partial \psi / \partial \bar{y}) \quad \rho \bar{v} = -\rho (\partial \psi / \partial \bar{s})$$

we have

$$u = (\partial \psi / \partial y) \quad v = -(\partial \psi / \partial s) \quad (2)$$

which serves to define the transformed velocities  $u$  and  $v$ .  $\psi$  automatically satisfies the continuity equation, and the zero streamline  $\psi = 0$  coincides with the  $x$  axis ( $y = 0$ ).

To reduce the problem to its simplest elements, the approximations are made so that the density-viscosity product  $\rho\mu$  is constant and the Prandtl number is unity. The continuity, momentum, and energy equations in the transformed

variables ( $s, y, u, v$ ) are now identical to their incompressible form:

$$(\partial u / \partial s) + (\partial v / \partial y) = 0 \quad (3)$$

$$u(\partial u / \partial s) + v(\partial u / \partial y) = \nu (\partial^2 u / \partial y^2) \quad (4)$$

$$u(\partial H / \partial s) + v(\partial H / \partial y) = \nu_e (\partial^2 H / \partial y^2) \quad (5)$$

where  $\nu_e$  is the kinematic viscosity ( $\mu / \rho$ ). Equations (4) and (5) indicate that  $H = A + Bu$  is a solution of the energy equation (5), where  $A$  and  $B$  are constants. This solution is admissible only if the initial and boundary conditions permit. The momentum equation (4) is now independent of the energy equation (5).

## Two-Layer Method

One method of solution is to integrate the equations numerically, starting with an assumed velocity profile at  $s = 0$ . The calculation is continued until a similar profile corresponding to  $s \rightarrow \infty$  is reached. This technique was used by Denison and Baum.<sup>8</sup> The approximate solution adopted here is to represent the velocity profile by a simple analytic function containing several parameters that are allowed to vary with  $s$ . By multiplying the  $s$  momentum equation by  $u^j$  ( $j = 0, 1, 2, \dots$ ) and integrating across the shear layer, coupled ordinary differential equations are obtained which describe the variation of the velocity profile parameters in the  $s$  direction. Boundary conditions are also applied at the extremities of the shear layer. The total number of boundary conditions and moment equations must be equal to the number of parameters appearing in the velocity profile.

In the present problem, however, the initial velocity profile is so radically different from subsequent profiles that it is difficult to represent the velocity profile as a whole by a single expression. Hence, the shear layer is divided into two layers: region I,  $y > 0$ ; and region II,  $y < 0$ . The velocity profile in each layer is assumed to be of the form:

Region I

$$\frac{u}{u_*} = f = A_0 + e^{-\sigma\eta} \sum_{k=0}^m a_k \eta^k \quad \eta = \frac{y}{\delta_1} \quad (6)$$

Region II

$$\frac{u}{u_*} = g = B_0 + e^{\sigma\eta} \sum_{k=0}^n b_k \eta^k \quad \eta = \frac{y}{\delta_2} \quad (7)$$

$$u(s) = u_*(s) \text{ along } \psi = y = 0$$

and  $\sigma = 0$  or  $1$  depending upon the type of representation that is desired. The number of terms ( $m, n$ ) are chosen so that the resulting profile will provide a "good approximation"

Received August 5, 1963; revision received January 31, 1964. The work discussed in this paper was carried out under the sponsorship and with the financial support of the U. S. Army Research Office and the Advanced Research Projects Agency, Contract No. DA-31-124 ARO(D) 33. This research is a part of Project DEFENDER sponsored by the Advanced Research Projects Agency. The authors wish to express their appreciation to Lester Lees and Barry Reeves of the California Institute of Technology for many fruitful discussions of this problem.

\* Associate Professor of Aeronautics, Firestone Flight Science Laboratory, Graduate Aeronautical Laboratories, Member AIAA.

† National Science Foundation Fellow, Firestone Flight Science Laboratory, Graduate Aeronautical Laboratories. Presently Assistant Professor, Department of Aerospace Engineering Sciences, University of Colorado, Boulder, Colo. Member AIAA.

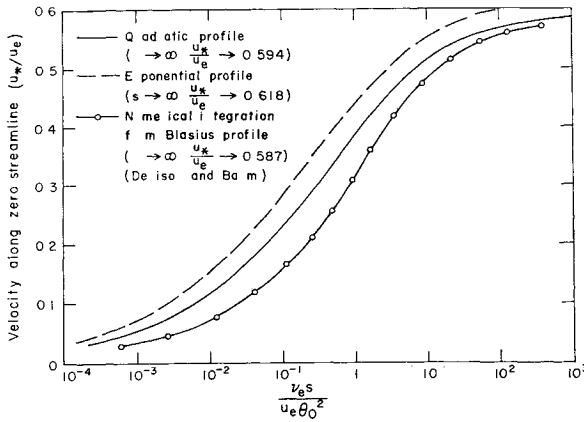


Fig. 1 Effect of shear layer profile on velocity along zero streamline

for the physical problem being considered<sup>‡</sup>. The profile parameters ( $A_0$ ,  $a_k$ ,  $B_0$ ,  $b_k$ ,  $\delta_1$ ,  $\delta_2$ ) are determined by the boundary conditions at the upper and lower extremities of the shear layer, the matching conditions at  $y = 0$ , and the moment equations. The possible boundary conditions are:

Outer Boundary

$$\begin{aligned} \sigma &= 0 & \eta &= 1 & & = 1, f' = f'' = & = 0 \quad (8) \\ \sigma &= 1 & \eta &\rightarrow \infty & & & \end{aligned}$$

Inner Boundary

$$\begin{aligned} \sigma &= 0 & \eta &= -1 & & g = 0, g' = g'' = 0 \quad (9) \\ \sigma &= 1 & \eta &\rightarrow -\infty & & \end{aligned}$$

(Primes denote derivatives of  $f$  with respect to  $\eta$  and derivatives of  $g$  with respect to  $\eta$ ). By demanding continuity of the velocity and its derivatives at  $y = 0$ , the following matching conditions are obtained:

$$(\partial f / \partial \eta)_0 = (\delta_1 / \delta_2) (\delta g / \delta \eta)_0 \quad r = 0, 1, 2, \quad (10)$$

### Solution for a Quadratic Profile

A very simple example of this method is a quadratic profile. Let  $\sigma = 0$ ,  $m = n = 2$ , so that the eight unknowns are  $\{a_0, a_1, a_2, b_0, b_1, b_2, \delta_1, \delta_2\}$ . The momentum integral equations are

$$\frac{d}{ds} \left[ \delta_1 \int_0^1 f(1-f) d\eta \right] = \frac{\nu_e f'(0)}{\delta_1 u_e} \quad (11)$$

$$\frac{d}{ds} \left[ \delta_2 \int_{-1}^0 g^2 d\eta \right] = \frac{\nu_e g'(0)}{\delta_2 u_e}$$

Define the initial thickness  $\delta_0$  and the quantities  $\lambda$  and  $\delta$  by  $\lambda = 1 - (u^*/u_e)$  and  $\delta = \delta_1 + \delta_2$ , where the limit  $s \rightarrow 0$  corresponds to  $\lambda \rightarrow 1$  and  $\delta \rightarrow \delta_1(s=0) \equiv \delta_0$ . Then the quadratic profiles satisfying the boundary and matching conditions  $r = (0, 1)$  are

$$f = 1 - \lambda(1 - \eta)^2 \quad g = (1 - \lambda)(1 + \eta)^2 \quad (12)$$

<sup>‡</sup> One difficulty with the momentum integral method is that the number of terms taken to represent the velocity profile is arbitrary. In this case, there are two criteria that aid in this choice: 1) the assumed profile must correspond closely to the specified initial profile as  $s \rightarrow 0$ ; and 2) the final similar profile for  $s \rightarrow \infty$  must agree well with the exact solution obtained by Chapman<sup>9</sup>. Because of its simplicity, the free shear-layer problem represents an excellent test case for the momentum integral method, since various combinations of profile parameters, boundary conditions, and moment equations may be used without undue algebraic complication. Such an exhaustive examination, however, is not attempted in this investigation.

<sup>§</sup> The quantities  $a_0$  and  $b_0$  are redefined to include  $A_0$  and  $B_0$ .

Table 1 Shear rates expressed in normalized terms

	Blasius	Quadratic	Exponential
$(\theta_0/u_e)(\partial u/\partial y)_0$	0.2205	0.2267	0.5

and the thicknesses are related by  $\delta_1 = \lambda\delta$  and  $\delta_2 = (1 - \lambda)\delta$ . Substituting Eq. (12) into Eq. (11) and solving the resulting equations, we obtain

$$\begin{aligned} \frac{\nu_e s}{u_e \delta_0^2} &= \frac{1}{5} \frac{(1 - \lambda)^3}{(3 - 9\lambda + 4\lambda^2)^2} - \\ &\quad \frac{1}{55} \frac{(\lambda + 3)(1 - \lambda)}{(3 - 9\lambda + 4\lambda^2)} + \frac{4}{55} \frac{1}{(33)^{1/2}} \times \\ &\quad \left[ \log \left| \frac{8\lambda - 9 + (33)^{1/2}}{8\lambda - 9 - (33)^{1/2}} \right| + \log \left( \frac{(33)^{1/2} + 1}{(33)^{1/2} - 1} \right) \right] \quad (13) \end{aligned}$$

which has the asymptotic form  $\lambda = 0.406$  as  $s \rightarrow \infty$ . This result,  $(u^*/u_e) = 0.594$ , is extremely close to the exact value of 0.587 found by Chapman<sup>9</sup>. The initial profile is, of course, restricted to a quadratic with  $\lambda = 1$ . A more accurate solution would be one in which two or more free parameters are available to specify the initial profile; the important effect to the initial profile on the rate of growth of  $u^*$  would then be apparent immediately.

### Solution for an Exponential Profile

The exponential profiles ( $\sigma = 1$ ) provide a particularly simple system of matching relations. Because of the fact that all derivatives of  $u$  approach zero at  $\pm \infty$ , the unknown parameters ( $\delta_1$ ,  $\delta_2$ ,  $a_k$ ,  $b_k$ ) are determined only by the matching conditions at  $y = 0$  and the moment equations  $M_r(\pm \infty)$ .

The velocity profiles for  $\sigma = 1$  and  $m = n = 0$ , satisfying the matching conditions  $r = 0, 1$ , are  $y > 0, f = 1 - \lambda e^{-\eta}$ ;  $y < 0, g = (1 - \lambda)e^{\eta}$ ; and the shear layer thicknesses are related by  $\lambda\delta_2 = (1 - \lambda)\delta_1$ . Substituting this velocity profile into Eq. (13) [using appropriate limits of integration], the solution is found to be

$$\begin{aligned} \frac{\nu_e s}{u_e \delta_0^2} &= \frac{3}{20} + \frac{(4\lambda - 1)}{20X} + \frac{\lambda(1 - \lambda)}{4X^2} + \\ &\quad \frac{3}{10(5)^{1/2}} \left[ \log \left| \frac{2\lambda - 3 + 5^{1/2}}{2\lambda - 3 - 5^{1/2}} \right| + \log \left| \frac{1 + 5^{1/2}}{1 - 5^{1/2}} \right| \right] \quad (14) \\ X &= 1 - 3\lambda + \lambda^2 \end{aligned}$$

whereas the similarity form for the shear layer thickness is

$$\lim_{s \rightarrow \infty} (\delta/x)(Re)^{1/2} = 4.10$$

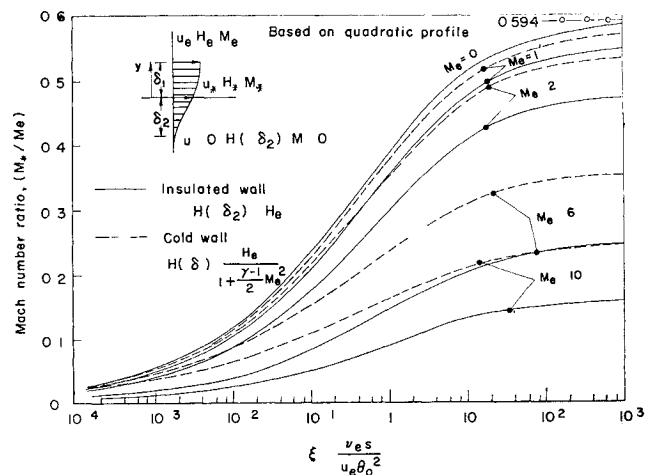


Fig. 2 Effect of Mach number and internal cooling on  $M^*$

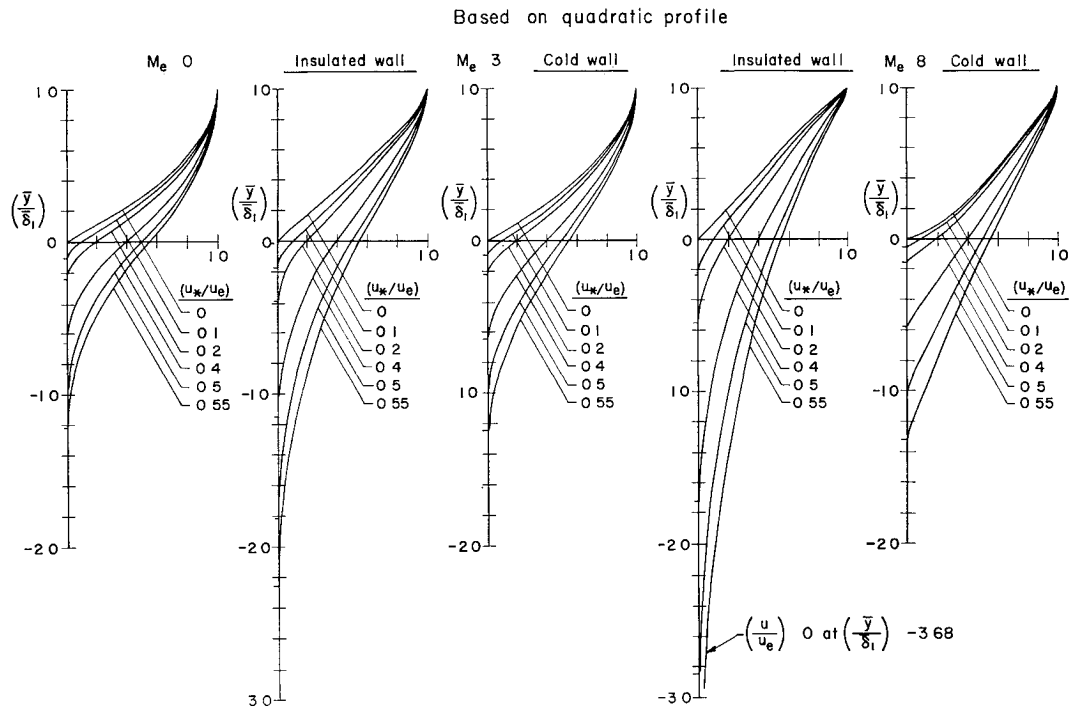


Fig 3 Velocity profiles in the compressible shear layer

and the asymptotic velocity ratio  $(u_*/u_e)$  is 0.618. This solution also contains a single profile parameter  $\lambda$ , so that the initial profile for  $s \rightarrow 0$  and  $\eta > 0$  is constrained to be  $(u/u_e) = 1 - \exp(-\eta)$ .

**Transformation to the Compressible Plane and Comparison with Numerical Solutions**

The initial momentum thicknesses in the incompressible and physical coordinates are identical in form, namely,

$$\bar{\theta}_0 = \int_0^\infty \left( \frac{\rho \bar{u}}{\rho \bar{u}_e} \right) \left( 1 - \frac{\bar{u}}{\bar{u}_e} \right) d\bar{y} = \int_0^\infty \left( \frac{u}{u_e} \right) \left( 1 - \frac{u}{u_e} \right) dy = \theta_0 \tag{15}$$

It is for this reason that the momentum thickness appears to be the “proper” length scale of the initial profile. The unbarred form of  $\theta_0$  will be used in a subsequent discussion.

The quadratic profile is found to give  $\bar{\theta}_0 = \frac{2}{15}\delta_0$ , and for the simple exponential profile  $\theta_0 = \frac{1}{2}\delta_0$ . For the numerical solution of Denison and Baum,<sup>8</sup> which uses a Blasius initial profile, the streamwise coordinate  $s^*$  is related to the present solutions by the equation<sup>10</sup>

$$s^* = 0.4863(\nu s/u_e \theta_0^2) \tag{16}$$

The variation of the mixing velocity  $u_*$  with the “proper” distance variable  $\xi = (\nu s/u_e \theta_0^2)$  is shown in Fig 1. The quadratic, exponential, and Blasius results are seen to be in qualitative agreement, although the magnitude of  $u_*$  differs

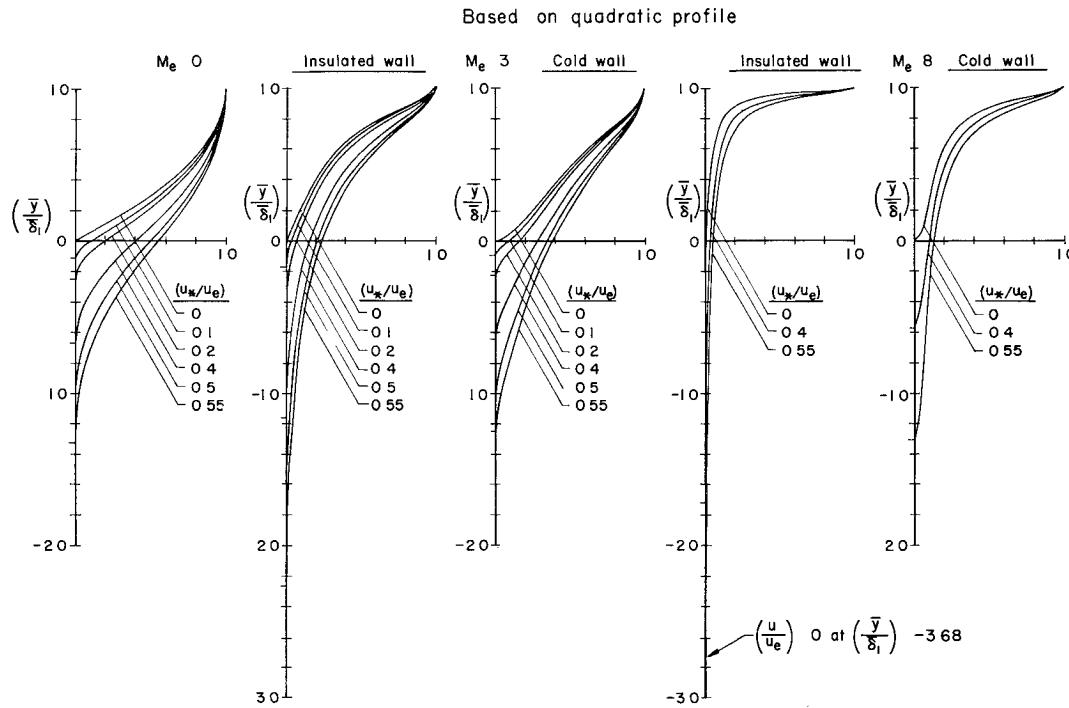


Fig 4 Mass-flow profiles in the compressible shear layer

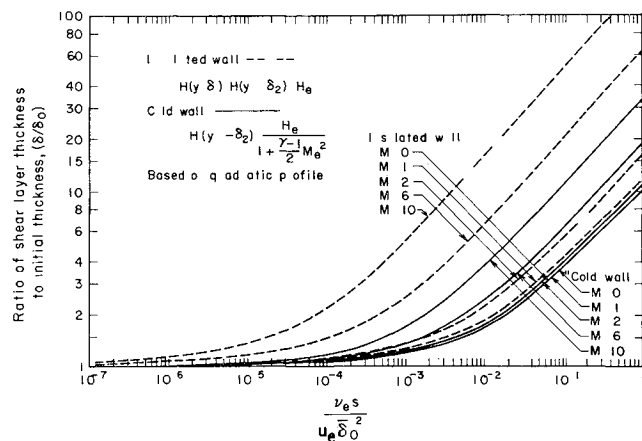


Fig 5 Effect of external Mach number and internal cooling on physical shear layer thickness

by as much as 0.15 at a given value of  $\xi$ . Even more disturbing is the fact that the values of  $\xi$  for a given  $u_*$  may differ by as much as a factor of 6. Since each of the solutions involves only one free profile parameter, it may not be stated with certainty whether the differences between the numerical solution and the moment method results are produced by the differences in the initial profile or the differences in the method of calculation.

However, near  $\xi = 0$ , the situation is quite clear. Each initial profile is linear near  $y = 0$ , so that the initial shear  $(\partial u / \partial y)_{y=0}$  determines the variation of  $u_*(\xi)$  for small  $s$ . These shear rates are expressed in normalized terms as shown in Table 1.

From this table, it is obvious that the initial growth of  $u_*(\xi)$  will be more rapid if the initial profile is an exponential than if it is a quadratic; this supposition is borne out by Fig. 1. The difference between the initial shear  $(\theta_0/u_e)(\partial u / \partial y)_0$  of a Blasius profile and a quadratic is small; hence, the difference between the values of  $u_*(\xi)$  and for small  $\xi$  calculated by Denison and Baum<sup>8</sup> and the values found from the quadratic solution are attributed to the approximate nature of the momentum integral method. Considering the simplicity of the momentum integral method, the agreement is very good.

### Effects of Heat Transfer and Calculations of $M_*$

For purposes of illustration, we will consider only the solution obtained for the quadratic profile. Consider first the case where the temperature in the base flow region ( $u \rightarrow 0$ ) is equal to the total temperature of the inviscid flow (this will be called the "insulated wall" case). Then  $H = H_e$  through the shear layer and

$$T/T_e = 1 + [(\gamma - 1)/2] M_e^2 [1 - (u/u_e)^2] \quad (17)$$

If the fluid in the base flow region is very cold, then  $M_*$  will be large. For example, consider the base temperature to be equal to the static temperature  $T_e$  of the external flow (this will be called the "cold wall" case). Then the equation corresponding to (17) is

$$T/T_e = 1 + [(\gamma - 1)/2] M_e^2 [(u/u_e) - (u/u_e)^2] \quad (18)$$

The physical distance  $\bar{y}$  may be written as a function of the transformed distance  $y$

$$\bar{y} = \int_0^y \frac{T}{T_e} dy \quad (19)$$

The Mach number  $M_*(\xi)$  may be calculated from Eqs (13, 17, and 18) using the definition  $M_* = u_*/(\gamma R T_*)^{1/2}$ . The results of this computation are shown in Fig. 2. Mass-flow and velocity profiles are shown in Figs. 3 and 4. In Fig. 5, the physical shear layer thickness is shown as a func-

tion of the streamwise coordinate  $(\nu s / u \delta_0^2)$ . These four figures lead to the following conclusions:

1) The Mach number  $M_*$  increases with increasing  $M$ , but this increase becomes small as  $M_e$  becomes large.

2) At higher Mach numbers, say  $M \gtrsim 6$ , the difference between the values of  $M_*$  for the cold wall and insulated wall cases may be 50% or more. In applying these results to the near wake of a body at high speeds, one common assumption<sup>11</sup> is that the turning of the shear layer at the neck of the wake is determined by the pressure rise  $(p' - p)$  required to bring the fluid along the zero streamline to rest by an isentropic compression process. This leads to the equation

$$\frac{p'}{p} = \left(1 + \frac{\gamma - 1}{2} M_*^2\right)^{\gamma/(\gamma - 1)}$$

The strong effect of base cooling on the dynamics of the near wake is therefore evident.

3) The velocity and mass-flow profiles in the shear layer exhibit the same compressible-incompressible relation as the corresponding profiles for a boundary layer. As  $M_e$  increases, the velocity profile in the physical plane becomes more linear. The mass-flow profile becomes less full with increasing  $M_e$ , and for the "insulated wall" temperature boundary condition, the mass flow below the zero streamline ( $y < 0$ ) is small.

4) The shear layer penetrates more and more deeply into the region below the zero streamline as  $M$  increases. Although the quadratic profile does not give a highly accurate description of the details of the profiles in the region of small velocity, it demonstrates qualitatively the large increase in total shear layer thickness with increasing Mach number.

5) The use of a "proper" length scale for the characteristic thickness of the initial shear is important. In Figs. 1 and 2, the momentum thickness  $\theta_0 \equiv \theta_0$  is used to define the streamwise coordinate  $\xi = (\nu s / u \theta_0^2)$ . Figure 2 shows that the Mach number ratio  $(M_*/M)$  achieves one half the value for  $\xi \rightarrow \infty$  at about  $\xi \cong 0.2$ , and this result is independent of  $M_e$  and  $H(-\delta_2)$ . An equivalent result is found for the growth of the shear layer velocity thickness  $\delta = \delta_1 + \delta_2$ . However, if  $\delta$  is plotted as a function of  $(\nu s / u \delta_0^2)$  as in Fig. 5, the value of the streamwise coordinate for which  $(\delta/\delta_0)$  approaches the similarity law  $(\delta/\delta_0) \sim (\nu s / u \delta_0^2)^{1/2}$  varies both with  $M$  and  $H(-\delta_2)$ .

### References

- 1 Crocco, L. and Lees, L., "A mixing theory for the interaction between dissipative flows and nearly isentropic streams," *J. Aeronaut. Sci.* **19**, 649-676 (1952).
- 2 Glick, H. S., "Modified Crocco-Lees mixing theory for supersonic separated and reattaching flows," *J. Aerospace Sci.* **29**, 1238-1249, 1259 (1962).
- 3 Tani, I., "On approximate solution of the laminar boundary layer equations," *J. Aeronaut. Sci.* **21**, 487-504 (1954).
- 4 Carlson, W. O., "Heat transfer in laminar separated and wake flow regions," *Proceedings of the 1959 Heat Transfer and Fluid Mechanics Institute* (Stanford University Press, Stanford, Calif., 1959) pp. 140-155.
- 5 Lees, L. and Reeves, B. L., "Some remarks on integral moment methods for laminar boundary layers with application to separation and reattachment," *Separated Flows Research Project, Graduate Aeronautical Labs., California Institute of Technology TR 1* (December 31, 1961).
- 6 Rom, J., "Theory for supersonic, two-dimensional laminar base-type flows using the Crocco-Lees mixing concepts," *J. Aerospace Sci.* **29**, 963-965 (1962); also Rom, J. and Victor, M., "Correlation of the base pressure behind a two-dimensional backward-facing step in a laminar supersonic flow," *TAE (Israel) Rept. 23* (December 1962).
- 7 Savage, S. B., "The effect of heat transfer on separation of

¶ The pressure  $p$  is the static pressure along the outer edge of the shear layer, and  $p'$  is the static pressure downstream of the neck of the wake.

laminar compressible boundary layers," Separated Flows Research Project, Graduate Aeronautical Labs California Institute of Technology TR 2 (June 1, 1962)

<sup>8</sup> Denison, M. R. and Baum, E., "Compressible free shear layer with finite initial thickness," AIAA J. 1, 342-349 (1963)

<sup>9</sup> Chapman, D. R., "Laminar mixing of a compressible fluid," NACA Rept 958 (1950)

<sup>10</sup> Dewey, C. F., Jr., "Measurements in highly dissipative

regions of hypersonic flows Part II The near wake of a blunt body at hypersonic speeds," Ph D Thesis, California Institute of Technology (1963)

<sup>11</sup> Chapman, D. R., Kuehn, D. M., and Larson, H. K., "Investigation of separated flows in supersonic and subsonic streams with emphasis on the effect of transition," NACA Rept 1356 (1958); this report supersedes NACA TM A55L14 (1956) and NACA TM 3869 (1957)

APRIL 1964

AIAA JOURNAL

VOL 2, NO 4

## A Study of Wakes behind a Circular Cylinder at $M = 5.7$

JOHN F. MCCARTHY JR. \*

*North American Aviation, Inc., Downey, Calif*

AND

TOSHI KUBOTA†

*California Institute of Technology, Pasadena, Calif*

The flow field behind a circular cylinder was investigated experimentally at a nominal Mach number of 5.7, over a range of Reynolds numbers from 4500 to 66,500, based on the cylinder diameter. Pitot pressure, static pressure, and total temperature were measured at various distances behind three cylinders of different diameters in order to determine the flow properties in the wake. The data at different Reynolds numbers were correlated in a manner indicated by a linearized theory for the laminar far wake with axial pressure gradient. Transition from laminar to turbulent flow was determined from the velocity profiles and correlated with results obtained from mass-diffusion and hot-wire fluctuation measurements.

### Nomenclature

$d$	= cylinder diameter
$h$	= static enthalpy
$M$	= Mach number
$p$	= static pressure
$p_0$	= freestream stagnation pressure, absolute
$p_{0g}$	= freestream stagnation pressure, gage
$p_p$	= pitot pressure
$Re_d$	= freestream Reynolds number based on cylinder diameter
$Re_x$	= Reynolds number based on distance along wake and conditions at edge of boundary layer
$Re_T$	= Townsend Reynolds number
$T_{aw}$	= adiabatic wire temperature
$u$	= component of velocity parallel to wake centerline
$v$	= component of velocity normal to wake centerline
$w$	= velocity defect, $1 - (u/u_\infty)$
$x$	= length along wake centerline measured from center of cylinder
$y$	= length normal to wake centerline measured from line through center of cylinder
$\epsilon_T$	= turbulent diffusivity
$\omega$	= angle of cylinder measured from stagnation point

### Subscripts

$e$	= conditions at outer edge of wake
$m$	= measured
$0$	= initial conditions (usually taken at wake neck)

### Introduction

THE nature of wakes is one of the oldest basic problems in the field of classical fluid mechanics. Although the wakes in low-speed flow have been discussed in several treatises,<sup>1-6</sup> it was only recently that research was directed toward the phenomenon of high-speed flow. The development of intercontinental ballistic missiles and hypersonic entry vehicles has kindled this interest in high-speed wakes.

The theoretical problem of hypersonic wakes was first treated by Feldman,<sup>7</sup> who devised a simple model of the wake flow. Feldman's basic approach has been extended by Lykoudis.<sup>8</sup> More recently, Lees and Hromas<sup>9</sup> have attacked the problem of turbulent diffusion in the wake by using integral methods to solve the boundary-layer equations. The two-dimensional laminar hypersonic wake with streamwise pressure gradient has been solved by Kubota,<sup>10</sup> using linearized equations.

Perhaps the major obstacle in correlating theory and experiment in hypersonic wakes is the difficulty of obtaining reliable and detailed experimental data. Atmospheric entry involves a range of temperature and Mach number that cannot be simulated effectively by known devices for extended periods. Therefore, only limited data have been secured, either from short-duration experimental facilities, such as ballistic ranges<sup>11</sup> and shock tunnels<sup>12</sup> or from actual flight where results are not easily duplicated. The conventional wind tunnel does not simulate the high Mach

Received June 6, 1963; revision received January 28, 1964. The work discussed in this paper was carried out under the sponsorship and with the financial support of the U. S. Army Research Office and the Advanced Research Projects Agency, Contract No. DA-04-495 ORD-3231. This research is a part of Project DEFENDER sponsored by the Advanced Research Projects Agency. This work also was supplemented by the Space and Information Systems Division of North American Aviation, Inc.

\* Director, Apollo Control Systems, Space and Information Systems Division. Associate Fellow Member AIAA.

† Associate Professor of Aeronautics. Member AIAA.